# DISSOCIATIVE AUTOIONIZATION AS A MECHANISM FOR THE PROTON FORMATION FROM METHANE AND METHANE-$d_4$ BY LOW ENERGY ELECTRON IMPACT

R. LOCHT, J.L. OLIVIER and J. MOMIGNY

*Institut de Chimie, Département de Chimie Générale et Chimie-Physique, Sart-Tilman par B-4000 Liège 1, Belgium*

## Abstract

The ion energy distribution and the electroionization efficiency curves of $H^+$ and $D^+$ from methane and methane-$d_4$ have been examined. The existence of thermal ions is unambiguously evidenced and the two lowest appearance thresholds of $H^+$ are measured at $(21.3 \pm 0.3)$ eV and $(22.17 \pm 0.1)$ eV. At both energies the protons have to be formed through dissociative autoionization. The present results closely parallel those of the dissociative excitation experiments on methane. The Jortner-Rice model for dissociation of polyatomic molecules is invoked to account for both the appearance of $H^+$ and high-Rydberg H atoms from $CH_4$.

## 1. Introduction

For a long while most of the attention has been payed to the fragmentation of methane into its most heavy ionized fragments; only scarce experimental work has been devoted to the proton formation.

Smith [1] measured the threshold energy of the proton formed by dissociative electroionization of methane and Fuchs and Taubert [2] analyzed the proton energy distribution observed for 75 eV electrons. Using the same technique Appell and Kubach [3] measured the appearance energy of protons from $CH_4$ for different initial kinetic energies. The dissociative excitation by electron impact of methane into metastable or high-Rydberg H atoms has extensively been examined by Finn et al. [4] and Donohue et al. [5]. These authors determined the excitation functions for the appearance of H* atoms, for the Lyman α emission of H* fragments and their kinetic energy distribution as a function of the electron energy. Using low energy electron impact, Oertel [6] measured the excitation function for Lyman α, β and γ emission from H* atoms produced by dissociative excitation of methane. Recently, initial kinetic energy distributions of $H^+$ obtained by 1 MeV ion impact on $CH_4$ have been reported by Edwards et al. [7]. The only dissociative photoionization work has been publish-ed by Kronebusch and Berkowitz [8]. Backx et al. [9] measured the mass spectrum of $CH_4$ as a function of the electron energy loss for high-energy primary electrons and gave the branching ratio for $H^+$ .

In the dissociative electroionization results reported up to now concerning the $H^+$ formation from $CH_4$, several discrepancies arise for both the lowest appearance energy of $H^+$ from methane and some results about the kinetic energy distribution of protons. Because of this unclear situation, the aim of this work is to reexamine the ionization efficiency curves as well as the ion energy distribution as a function of the impinging electron energy for $H^+$ and $D^+$ from $CH_4$ and $CD_4$ respectively.

## 2. Experimental

The experimental setup used in the present work has fully been described elsewhere [10]. Briefly, the ions formed in a conventional Nier type ion source are focussed on an exit hole, energy analyzed by a retarding lens and mass selected in a quadrupole filter. The ion current collected on a Cu-Be electron multiplier, is continuously scanned as a function of either the electron energy at fixed retarding potential or the retarding potential at fixed electron energy. Both signals are electronically differentiated, stored and averaged in a multichannel analyzer and plotted on a *X-Y* recorder.

Unless otherwise stated the operating conditions maintained in the course of this work are identical to those described elsewhere [10]. The methane gas, purchased from Air Liquide of 99.995 % as well as the methane-$d_4$ from Merck Sharp and Dohme of 99 % isotopic purity were used without further purification. The

ultimate vacuum is 4 x $10^{-8}$ Torr and the signal corresponding to the $H_2O$ ion is less than 0.1 % of the $CH_4^+$ ion intensity in the same conditions. The pressure of $CH_4$, when not other-wise stated, is of 3 x $10^{-7}$ Torr and the intensity of the ionizing electron beam is 1 $\mu A$.

For the kinetic energy scale calibration the maximum of the first differentiated retarding curve of the $CH_4^+$ ion is used as the zero energy point. The same reference is used when the ionization efficiency curves are recorded at different values of the retarding potential. The first adiabatic ionization potential of $CH_4$ at 12.61 eV [11] (and 12.88 for $CD_4$ [12]) measured by linear extrapolation [10] of the first differentiated ionization efficiency curve of $CH_4^+$, is used for the electron energy scale calibration.

Ion energy distributions were recorded at least five times at all mentioned electron energies while the appearance energies are averaged values of five independent measurements.

## 3. Results

Typical ion energy distributions recorded for $H^+$ formed by dissociative ionization of $CH_4$ by the impact of electrons of energies ranging from 25-50 eV are shown in fig. 1. The position of the maxima are measured at $0.0 \pm 0.01$ eV, $0.50 \pm 0.05$ eV, $0.9 \pm 0.05$ eV, $2.35 \pm 0.05$ eV and $3.97 \pm 0.03$ eV. To ensure that the $H^+$ ion energy distribution is not perturbed by any trace of $H^+$ ions formed by dissociative ionization of $H_2O$, the energy distribution of $D^+$ from $CD_4$ has been recorded and corn pared with the proton produced by $CH_4$. Fig. 2 shows a typical recording of the two $H^+/CH_4$ and $D^+/CD_4$ distributions both obtained for 75 eV electrons. The ion energy distributions of $H^+$ and $D^+$ have been further examined close to the thresh-old of appearance of these ions. Fig. 3 shows the results for $D^+$ from $CD_4$ obtained for 22-25 eV electrons. In these distributions two well resolved peaks are present: (i) the thermal peak which remains at 22 eV and (ii) the 2.35 eV peak for which the appearance energy is in the electron energy range of 22-23 eV. This peak also shows a *constant fwhm over the electron energy range of 23-25 eV*. This last feature has been noticed earlier by Appell and Kubach [3] for $H^+$ and by Donohue et al. [5] for high-Rydberg H atoms.

Fig. 4 shows typical first differentiated ionization efficiency curves of $H^+$ and $D^+$ from $CH_4$ and $CD_4$ obtained for a retarding potential $V_R = 0$ V. Both results illustrated in figs. 2 and 4 clearly show the absence of any detectable contribution of $H^+$ from $H_2O$ in the present experiment. Moreover, a contribution of $H^+$ from $H_2O$ would lower the first threshold to 18.7 eV [13, 14]. In fact the first thresh-old observed for $H^+$ from $CH_4$ and $D^+$ from $CD_4$ is measured at $21.3 \pm 0.3$ eV and $21.2 \pm 0.4$ eV, respectively. The second onset energy is at $22.17 \pm 0.1$ eV in both cases. Two other thresholds are observed at $28.0 \pm 0.4$ eV and $29.8 \pm 0.2$ eV. The existence of the third threshold is evidenced in the second differentiated ionization efficiency curve shown in fig. 5. The linear extrapolation in this curve would lower the two last thresholds to better values, i.e. $26.8 \pm 0.4$ eV and $28.7 \pm 0.2$ eV, respectively.

The dependence of the appearance energy of $H^+$ upon the retarding potential is illustrated in fig. 6. The results obtained by increasing the retarding potential stepwise by 0.2 V are summarised in the kinetic energy-versus-appearance energy plot shown in fig. 7 for the two first thresholds. The error bars represent the largest deviation from the average of five independent measurements.

## 4. Discussion

In the present paper we will restrict the discussion of our results to the two lowest thresholds for two reasons : (i) large discrepancies have to be noticed in the previously reported results for both the ion energy distribution and the appearance energy of $H^+$ and (ii) the energy of the two thresholds lie in between the range of the two first ionization potentials where most of the data about $CH_4$ are available.

### 4.1. Proton energy distribution

Fuchs and Taubert [2], and Appell and Kubach [3] observed the proton energy distribution and measured maxima near 1 eV, 2.5 eV and around 4 eV in good agreement with our results. However, the last authors do not observe the existence of a thermal peak and the former explicitly mention the existence of "at least four groups of ions", one of which lies at or close to thermal energy. Appell [14] corrected the kinetic energy distributions and the ionization efficiency curves for the proton produced by dissociative ionization of residual water. To avoid this difficulty we used as mentioned above $CD_4$ and compared the results obtained for D

$^+$ with those of H$^+$ from CH$_4$ (see fig. 2).

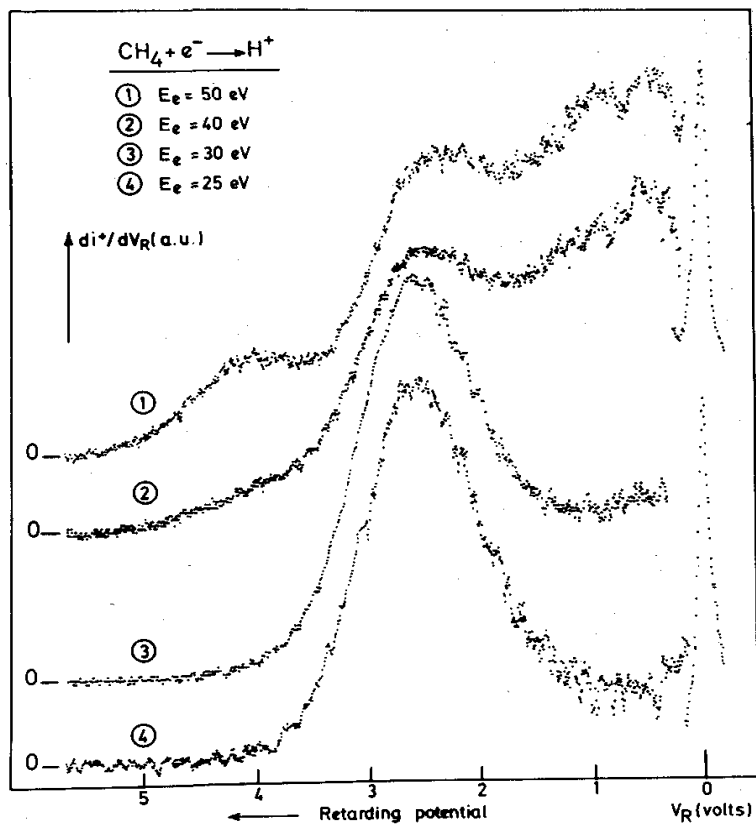**Fig. 1.** *Energy distribution of protons obtained in CH$_4$ for electron energies of 25 eV, 30 eV, 40 eV and 50 eV.*



**Fig. 2.** *H$^+$/CH$_4$ and D$^+$/CD$_4$ ion energy distribution at 75 eV electron energy.*
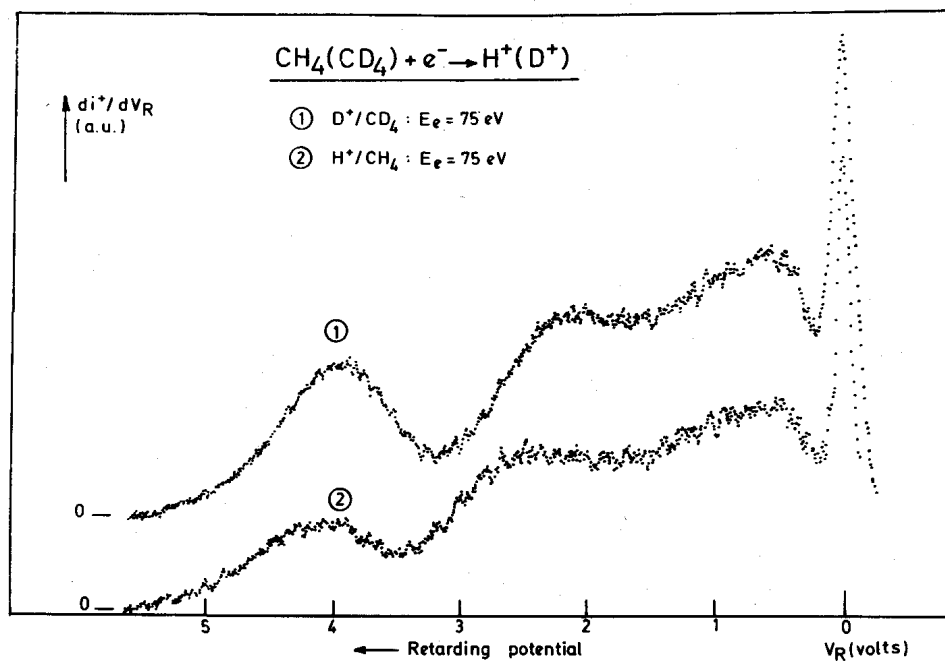
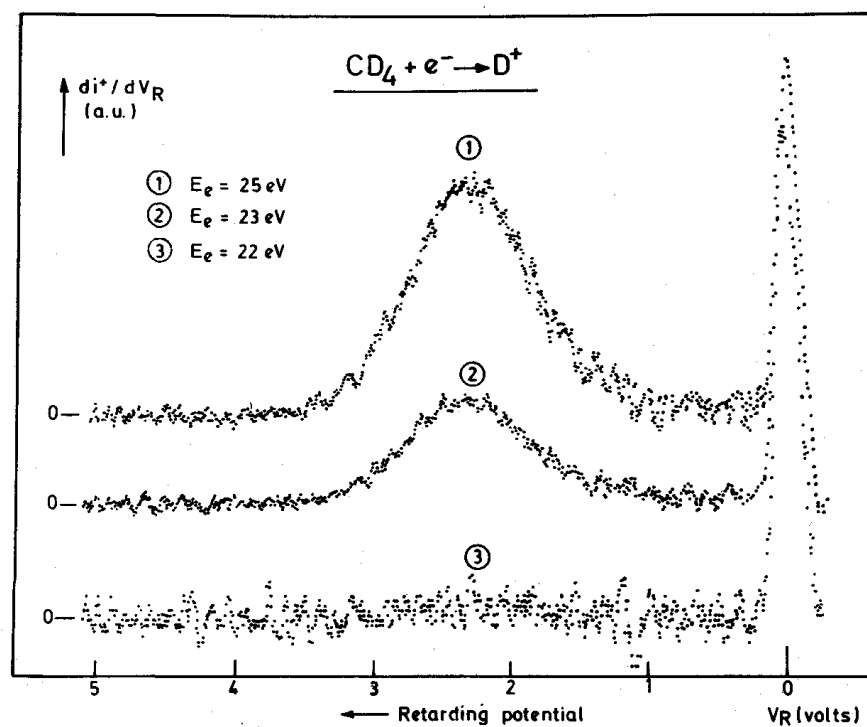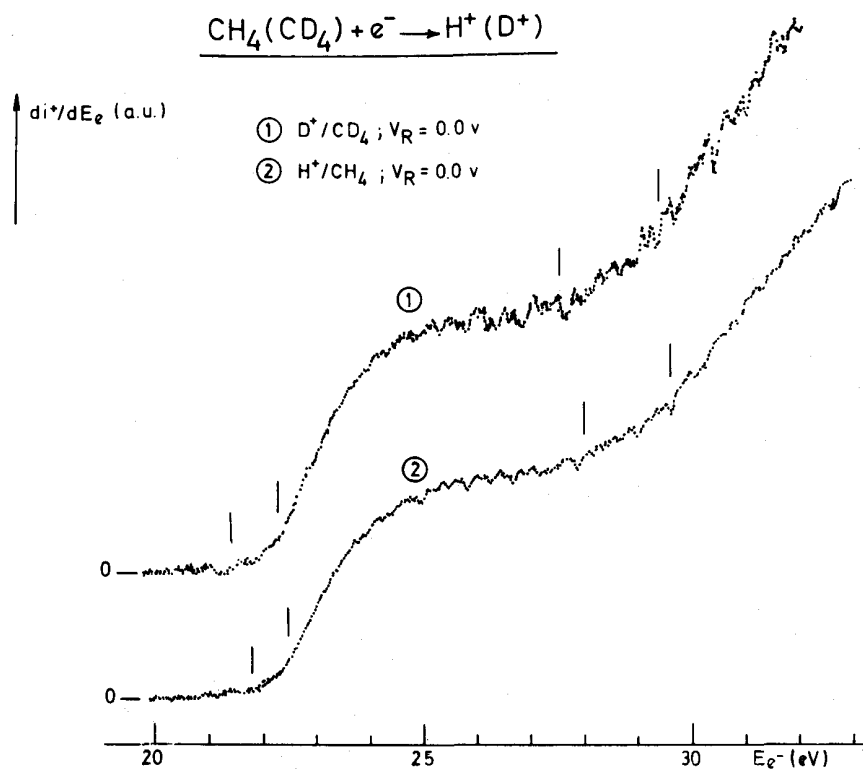**Fig. 3**. *$D^+/CD_4$ ion energy distribution obtained with 22 eV, 23 eV and 25 eV electrons.*



**Fig. 4.** *First differentiated ionization efficiency curves of $H^+/CH_4$ and $D^+/CD_4$ recorded at retarding potential $V_R$ = 0 V.*

Donohue et al. [5] observed the kinetic energy distribution of metastable and high-Rydberg H atoms produced by dissociative excitation of $CH_4$ by the impact of variable energy electrons. In these experiments maxima are also observed around 1 eV, 2.5 eV and 4 eV. These authors do not find any process at thermal or nearly thermal energy. They mention a weak process with an onset near 14 eV and a kinetic energy distribution extending up to 3.2 eV. This process has a quadratic dependence upon the electron beam intensity.

We examined the dependence of the proton energy distribution, observed for 30 eV electrons, upon the pressure of $CH_4$ in the ion source and the electron beam intensity. Both the intensity of the thermal peak and of the 2.35 eV peak *are first power dependent upon* the pressure of the target gas and upon the electron beam intensity which has been investigated over the 0.5-2 $\mu$A range.

**Fig. 5.** *First and second differentiated ionization efficiency curves of $H^+/CH_4$ at $V_R = 0$ V.*
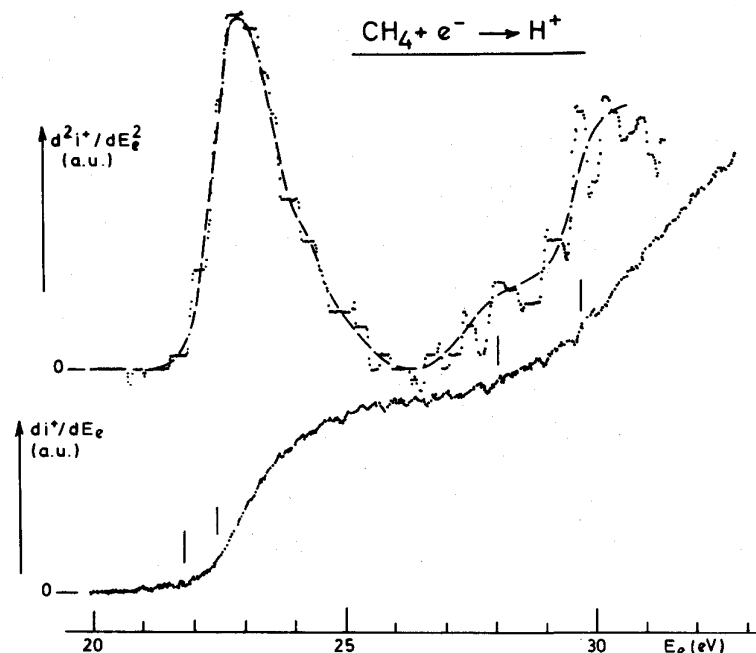


*4.2. Appearance energy*

Excepting the first process for $H^+$ production of fairly low cross section, the second threshold at 22.17 ± 0.1 eV compares fairly well to the first appearance energy determination of Smith [1] at 22.7 ± 0.5 eV. This author mentions a second onset at 29.4 ± 0.6 eV in good agreement with the second important increase in our first differentiated ionization efficiency curve at 29.8 ± 0.2 eV. In their dissociative ionization work Appell et al. [3, 14] measured the first appearance energy at 24.0 ± 0.5 eV. An overestimation of the contribution of the $H^+$ current from residual water might shift the lowest threshold to higher energies. The comparison of the ionization efficiency curves of $H^+$ and $D^+$ support this hypothesis (see fig. 4).

In dissociative excitation experiments, Finn et al. [4] measured two thresholds for metastable hydrogen fragments production at 22.0 ± 0.5 eV and 25.5 ± 0.6 eV. Donohue et al. [5] observed high-Rydberg H atoms from methane at 23.0 ± 0.5 eV, 24.5 ± 0.5 eV and 26.4 ± 0.5 eV. The same authors determined the excitation function for emission of H atoms in the $n = 4$ state. Onsets are determined at 22.0 ± 0.3 eV and 27.4 ± 0.5 eV. Oertel [6] measured the onsets for Lyman and Balmer emission by H* atoms from methane. By linear extrapolation Lyman $a, \beta$ and $\gamma$ have their onset at 21.4 ± 0.5 eV, 21.8 ± 0.5 eV and 22.1 ± 0.5 eV, respectively. A second threshold is observed at 25.3 ± 1.2 eV, 25.8 ± 1.2 eV and 25.8 ± 1.2 eV.

By dissociative photoionization Kronebusch et al. [8] have determined the mass spectrometric branching ratio for $H^+$ from methane as a function of the proton energy. A first onset is observed around 21 eV and a second sharp increase around 28 eV. In a very recent work Oertel et al. [15] measured the photoionization

efficiency curve of $H^+$ produced from methane using synchrotron radiation. A first steeply rising onset is measured at 22.2 eV. The second threshold is around 27 eV. Below 22 eV, the signal is obscured by the ionization of H atoms produced by the photolysis of methane. The mass spectrum of $CH_4$ measured by Backx et al. [9] as a function of the electron energy loss gives an information similar to that of Kronebusch et al. [8] obtained by photoionization

**Fig. 6.** *First differentiated ionization efficiency curves of $H^+/CH_4$ at various retarding potentials.*
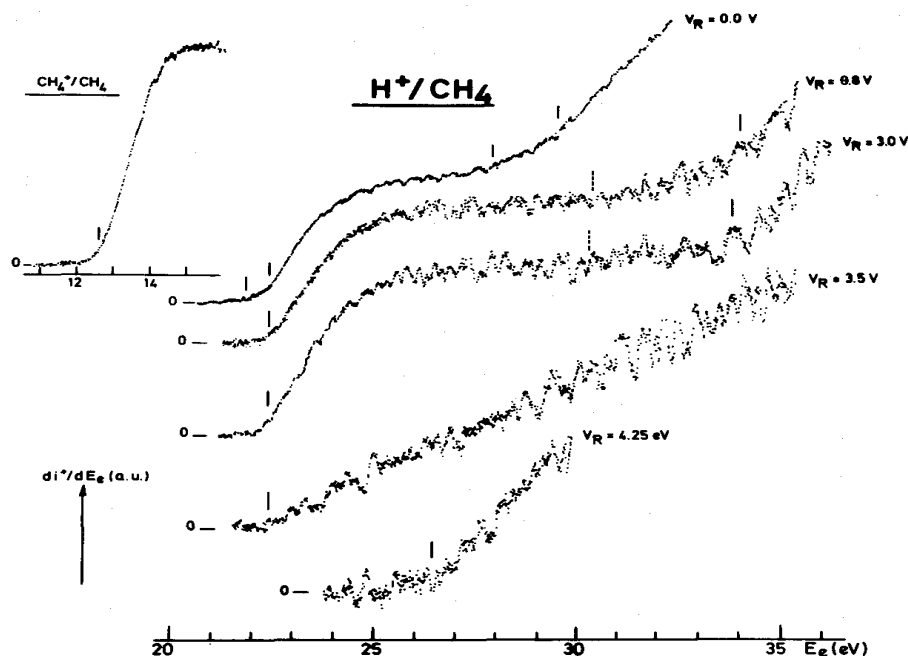


## 5. Interpretation

*The first process* with a threshold at $21.3 \pm 0.3$ eV gives only rise to protons carrying thermal and nearly thermal energy as it is clearly shown in fig. 3. This onset lies in the energy range where no ionization cross section is observed in the photo-electron spectrum of $CH_4$ [12]. The two first adiabatic ionization energies of $CH_4$ in the $\widetilde{X}\,^2T_2$ and $\widetilde{A}\,^2A_1$ states of $CH_4^+$ are observed at 12.615 eV [11] and 22.39 eV [12]. At this energy the protons have to be formed by dissociative autoionization through the process

$$CH_4 + e^- \rightarrow CH_4^* + e^-, \qquad (1)$$

$$CH_4^* \rightarrow CH_3(\widetilde{X}\,^2A_2'') + H^+ + e^-. \qquad (2)$$
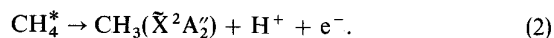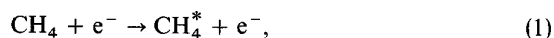
An indication for the existence of such an auto-ionizing state in the energy range of 21.3 eV could be found in a recent work published by Marmet et al. [16] who studied the electroionization efficiency curves of $CH_4^+$, $CH_3^+$ and $CH_2^+$ with monoenergetic electrons. For $CH_4^+$ and $CH_3^+$ they observe a well defined structure at 21.3 eV at the same energy measured for the first onset of $H^+$. It is likely that at 21.3 eV several autoionizing dissociation channels are open.

However the lowest dissociation limit is calculated at 18.1 eV [14] for the process

$$CH_4 + e^- \rightarrow CH_3(\widetilde{X}\,^2A_2'') + H^+ + 2e^-.$$
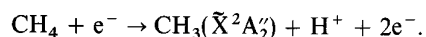
The energy difference of $21.3 - 18.1 = 3.2$ eV has to be converted into internal energy of the $CH_3$ radical.

The first known electronic excited state of $CH_3$ is $\widetilde{B}\,^2A'_1$ at 5.73 eV above the ground state [17]. An $\widetilde{A}$ $^2E'$ state lying between the $\widetilde{X}$ and $\widetilde{B}$ states has not been observed. A first interpretation of the onset at 21.3 eV could be

$$CH_4^* \rightarrow CH_3(\tilde{A}\,^2E') + H^+ + e^-, \qquad (2a)$$
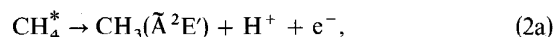
where the $^2E'$ state should be at 3.2 eV above the ground state of $CH_3$. Alternatively the energy difference of 3.2 eV could be entirely converted into vibrational energy of $CH_3$ in the ground electronic state

$$CH_4^* \rightarrow CH_3(\tilde{X}\,^2A_2'')_v + H^+ + e^-. \qquad (2b)$$
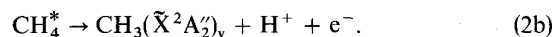
Finally within the limit of uncertainty on our measurements, we cannot exclude the formation of an ion pair

$$CH_4^* \rightarrow CH^- + H^+ + H_2 \qquad (2c)$$
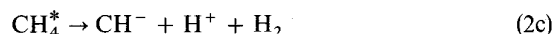
for which the threshold is calculated at 21.6 eV using the electron affinity EA(CH) = 1.24 eV [18]. This would however disagree with our earlier measurement of the onset of ion pair formation of $CH^-$ from $CH_4$ determined at $24.4 \pm 0.3$ eV [19].

*The second onset* measured at $22.17 \pm 0.1$ eV corresponds to a significant increase in the first differentiated ionization efficiency curve. The protons formed at this energy are related to the ion energy distribution which has the maximum at 2.35 eV and extends over the 0.8-3.5 eV range. As noticed earlier, this proton energy distribution peak has a *constant width* over an electron energy range from *threshold to 25 eV*. Furthermore fig. 7 shows that the'se protons have a constant appearance energy for retarding potentials of 0-3.5 eV. The measured appearance energy lies close to the second adiabatic ionization energy of $CH^+_4$ at 22.39 eV [12] for which the vibrational structure extends up to 24 eV. The formation of the protons at 22.17 eV by populating the $^2A_2$ state of $CH^+_4$ in its successive vibrational levels which subsequently predissociate could not account for the present experimental observations. At 22.17 eV the production of protons by direct dissociative ionization [3] is thus excluded.

The only process which can be invoked to interprete the proton formation at this energy is the dissociative autoionization mechanism such as reactions (1) and (2) where the superexcited states of $CH_4$ involved in the process at 22.17 eV lie close to the second ionization continuum. Its dissociative autoionization gives rise to protons with a constant ion energy distribution. This means that the excess energy of about 4.1 eV with respect to the lowest dissociation limit is converted into internal *and* translational energy of the fragments $CH_3$ and $H^+$.

**Fig. 7**. *Kinetic energy (t) versus appearance energy (AP) plot for $H^+/CH_4$ and $D^+/CD_4$ in the case of the two first thresholds respectively at 21.3 eV and 22.17 eV. The error bars indicate the largest deviation from the averaged onset value of five measurements.*
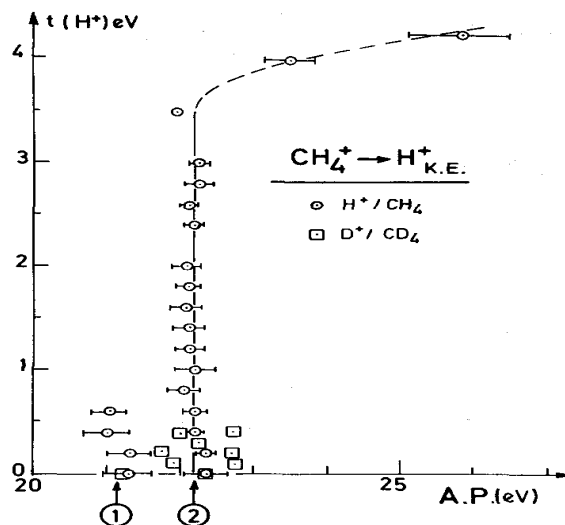


The most appropriate mechanism accounting for these results is the dissociation model of polyatomic molecules proposed by Jortner et al. [20]. In the frame of this model the system prepared in a defined vibronic state interacts with a quasi-continuum of vibrational levels. In the present case, the density of vibrational levels

for the $n$s, $n$p, $n$d Rydberg states of $CH_4$, including a vibrational distribution similar to that observed for the $^2A_1$ state of $CH_4^+$ to which they converge, has been evaluated to be of the order of 100/eV in the range of the observed threshold energy. Dissociation will occur when the quasi-continuum is coupled to the dissociation continuum. The dissociation rate will depend upon the value of the coupling matrix elements between the initial state and the quasi-continuum and the coupling between this quasi-continuum and the dissociation continuum.

The dissociative excitation results [4-6] observed in the energy range of 22-23 eV, which parallel very closely the results observed for the appearance of $H^+$, could be interpreted in the frame of the same model. At 22 eV the quasi-continuum of vibrational energy will competitively interact with the dissociation into neutral $CH_3$ and H* and/or a proton.

## Acknowledgement

## References

[1] L.G. Smith, Phys. Rev. 51 (1937) 263.

[2] R. Fuchs and R. Taubert, Z. Naturforsch. 19a (1964) 494.

[3] J. Appell and C. Kubach, Chem. Phys. Letters 11 (1971) 486.

[4] T.G. Finn, B.L. Carnahan, W.C. Wells and E.C. Zipf, J. Chem. Phys. 63 (1975) 1596.

[5] D.E. Donohue, J.A. Schiavone and R.S. Freund,J. Chem. Phys. 67 (1977) 759, 769.

[6] H. Oertel, Diplomarbeit, University Hamburg, Germany (1977).

[7] A.K. Edwards, J.E. Graves, R.M. Wood and M.F. Steuer, J. Chem. Phys. 69 (1978) 1985.

[8] P.L. Kronebusch and J. Berkowitz, Intern. J. Mass.Spectrom. Ion Phys. 22 (1976) 283.

[9] C. Backx, G.R. Wight, R.R. Tol and M.J. van der Wiel, J. Phys. B 8 (1975) 3007.

[10] R. Locht and J. Schopman, Intern. J. Mass.Spectrom. Ion Phys. 15 (1974) 361.

[11] W.A. Chupka and J. Berkowitz, J. Chem. Phys. 54(1971) 4256.

[12] C.R. Brundle, M.B. Robin and H. Basch, J. Chem.Phys. 53 (1970) 2196.

[13] H. Ehrhardt and A. Kresling, Z. Naturforsch. 22a (1967) 2036.

[14] J. Appell, Thesis, Paris (1972).

[15] H. Oertel and M. Kratzat, private communication.

[16] P. Marmet and L. Binette, J. Phys. B 11 (1978) 3707.

[17] G. Herzberg, Molecular spectra and molecular structure, Vol. 3, Electronic spectra and molecular structure of polyatomic molecules, (Van Nostrand, New York, 1966).

[18] A. Kasdan and E. Herbst, Chem. Phys. Letters 31 (1975) 78.

[19] R. Locht, Thesis, University of Liège, Belgium (1971).

[20] J. Jortner, S.A. Rice and R.M. Hochstrasser, Advan. Photochem. 7 (1969) 256 ff.